Published in final edited form as:
Cancer Cell. 2008 August 12; 14(2): 135–145. doi:10.1016/j.ccr.2008.07.003.

Medulloblastoma can be Initiated by Deletion of *patched* in Lineage-Restricted Progenitors or Stem Cells

Zeng-Jie Yang[1], **Tammy Ellis**[2], **Shirley L. Markant**[1], **Tracy-Ann Read**[1,3], **Jessica D. Kessler**[1], **Melissa Bourboulas**[2], **Ulrich Schüller**[4], **Robert Machold**[5], **Gord Fishell**[5], **David H. Rowitch**[6], **Brandon J. Wainwright**[2,*], and **Robert J. Wechsler-Reya**[1,*]

1 *Department of Pharmacology and Cancer Biology, Duke University Medical Center, Durham, NC*

2 *Institute for Molecular Bioscience, University of Queensland, St Lucia, Australia*

3 *Department of Biomedicine, University of Bergen, Bergen, Norway*

4 *Center for Neuropathology, Ludwig-Maximilians-Universität, Feodor-Lynen-Strasse 23, 81377 Munich, Germany*

5 *Smilow Neuroscience Program and Department of Cell Biology, NYU School of Medicine, New York, NY*

6 *Institute for Regeneration Medicine and Division of Neonatology, UCSF School of Medicine, San Francisco, CA*

SUMMARY

Medulloblastoma is the most common malignant brain tumor in children, but the cells from which it arises remain unclear. Here we examine the origin of medulloblastoma resulting from mutations in the Sonic hedgehog (Shh) pathway. We show that activation of Shh signaling in neuronal progenitors causes medulloblastoma by 3 months of age. Shh pathway activation in stem cells promotes stem cell proliferation, but only causes tumors after commitment to – and expansion of – the neuronal lineage. Notably, tumors initiated in stem cells develop more rapidly than those initiated in progenitors, with all animals succumbing by 3–4 weeks. These studies suggest that medulloblastoma can be initiated in progenitors or stem cells, but that Shh-induced tumorigenesis is associated with neuronal lineage commitment.

SIGNIFICANCE

The Shh pathway regulates growth of neural progenitors and stem cells, and activation of this pathway has been suggested to play a role in medulloblastoma and other brain tumors. We use conditional *patched* knockout mice to test the effects of Shh pathway activation in granule neuron precursors and stem cells. We demonstrate that both cell types can serve as cells of origin for medulloblastoma, and that the cell in which the tumor is initiated can have an important impact on the rate of tumor progression. Moreover, we show that deletion of *patched* in stem cells leads to medulloblastoma and not astrocytoma or oligodendroglioma, suggesting that the neuronal lineage may provide a critical context for the oncogenic effects of Shh signaling.

*Correspondence: rw.reya@duke.edu or b.wainwright@imb.uq.edu.au.

INTRODUCTION

The cell of origin for most types of cancer remains unknown. Identifying the normal cell that gives rise to a tumor is important because it allows studies of the normal cell to be used as a source of insight into the behavior of the tumor. Moreover, it allows for direct comparisons between tumor cells and their normal counterparts (e.g. using genomic or proteomic approaches), so that key differences and vulnerabilities of tumor cells can be identified. Finally, recent studies suggest that cells resembling the cell of origin may persist in mature tumors, and may be critical for propagating these tumors *in vivo*. If so, identifying the cell of origin may facilitate development of more effective approaches to therapy.

Our studies have focused on the cell of origin for medulloblastoma, a highly malignant tumor of the cerebellum. Medulloblastoma occurs most frequently in children between the ages of 5 and 10, but may occur in adults as well (Ellison, 2002; Packer et al., 1999). Despite important progress in treatment of the disease, the prognosis for many medulloblastoma patients remains bleak: almost half the patients who develop the disease die from it, and those who survive often suffer severe side effects from the treatment, including cognitive deficits, endocrine disorders and increased susceptibility to secondary tumors later in life (Heikens et al., 1998; Mulhern et al., 2005; Packer et al., 1999). Improved approaches for treating medulloblastoma are likely to come from a deeper understanding of its molecular and cellular origins.

The cell of origin for medulloblastoma has been the subject of debate for many years (Eberhart, 2007; Read et al., 2006). The morphology of tumor cells and their location on the surface of the cerebellum have led to speculation that the tumors arise from granule neuron precursors (GNPs), restricted progenitors that give rise only to granule neurons. In support of this view, immunohistochemical studies have demonstrated that medulloblastoma cells express markers commonly associated with GNPs, such as p75NTR, TrkC, Zic1 and Math1 (Buhren et al., 2000; Pomeroy et al., 1997; Salsano et al., 2004; Yokota et al., 1996). On the other hand, a variety of studies have shown that medulloblastomas can express stem cell markers and can differentiate into both neurons and glia (Hemmati et al., 2003; Singh et al., 2003), raising the possibility that these tumors may arise from multipotent neural stem cells (NSCs). More recently, it has been suggested that some subtypes of medulloblastoma may arise from stem cells and others from GNPs (Gilbertson and Ellison, 2008); however, definitive evidence for the cell of origin of any particular subtype of medulloblastoma remains elusive.

Although analysis of markers expressed by human medulloblastoma cells can provide clues to the cell of origin, such studies have significant limitations. In part, this is because the early stages of tumorigenesis are usually not detectable or accessible in human patients, so inferences about the cell of origin must be made retrospectively, based on the phenotype of cells from fully formed tumors. Since these cells may have changed dramatically during the course of tumorigenesis, expression of a particular marker in a tumor cell may not reflect the expression of this marker during development. In these respects, mouse models of medulloblastoma offer significant advantages for studying the origin of the disease.

One of the most powerful and widely studied models of medulloblastoma is the *patched* (*ptc*) mutant mouse (Goodrich et al., 1997; Oliver et al., 2005). *ptc* is an antagonist of the Shh signaling pathway, which functions as a critical regulator of both stem cells and progenitors in the CNS (Ahn and Joyner, 2005; Balordi and Fishell, 2007; Wechsler-Reya and Scott, 1999). Homozygous *ptc* knockouts have multiple defects in the neural tube, the heart and other tissues, and die early in embryogenesis (Goodrich et al., 1997). Heterozygotes from this strain survive, and approximately 15% of them develop cerebellar tumors that resemble human medulloblastoma (Goodrich et al., 1997; Oliver et al., 2005). Since *ptc* mutations have also been observed in many human medulloblastomas (Hahn et al., 1996; Johnson et al., 1996;

Raffel et al., 1997), these animals have become an important model for the disease. Studies of *ptc* mutant mice have provided insight into the early stages of tumorigenesis (Oliver et al., 2005), interactions between *ptc* and other tumor suppressor genes (Hahn et al., 2000; Wetmore et al., 2001; Zindy et al., 2007) and the utility of hedgehog pathway inhibitors as therapeutic agents for medulloblastoma (Romer et al., 2004; Sanchez and Ruiz i Altaba, 2005). However, because *ptc* is mutated in all cells in these animals (including NSCs and GCPs), they cannot be readily used to study the cell of origin.

To identify the cell of origin for *ptc*-associated medulloblastoma, we have taken advantage of a conditional allele of *ptc* (Adolphe et al., 2006; Ellis et al., 2003) that allows inactivation of the gene in either GNPs or NSCs. We show that deletion of *ptc* in GNPs results in a marked expansion of the EGL where granule cells develop. Although many *ptc*-deficient GNPs eventually stop dividing and differentiate into neurons, in each animal a cohort of GNPs continues to proliferate, and by 3 months of age, all mice develop tumors. Deletion of *ptc* in multipotent stem cells leads to expansion of the stem cell population, but only stem cells that commit to the granule lineage continue to divide and go on to form tumors. The increased production of GNPs (from the expanded stem cell pool) and the continued growth of these cells during postnatal development leads to rapid tumor formation, with 100% of animals succumbing to medulloblastoma by 3–4 weeks of age. These studies demonstrate that both progenitors and stem cells can respond to Shh signaling and can serve as cells of origin for medulloblastoma.

RESULTS

Math1-Cre/Ptc$^{C/C}$ mice allow deletion of *ptc* in GNPs

Mice heterozygous for mutations in *ptc* develop cerebellar tumors that resemble human medulloblastoma (Goodrich et al., 1997; Oliver et al., 2005). In these mice, *ptc* is inactivated in all cells (including GNPs and NSCs), so definitive conclusions about the cell of origin are not possible. To determine whether loss of *ptc* in GNPs can lead to medulloblastoma, we sought to create GNP-specific *ptc* knockout mice. To this end, we crossed two strains of mice: Math1-Cre transgenic mice (Schuller et al., 2007), which express Cre recombinase specifically in GNPs, and conditional *ptc* knockout (Ptc$^{C/C}$) mice (Adolphe et al., 2006; Ellis et al., 2003), which have loxP recombinase recognition sites flanking a portion of the *ptc* gene.

Math1-Cre mice were generated using a construct containing the Cre coding sequence downstream of a 1.4 kb Math1 enhancer element that has been used previously to express transgenes in GNPs (Machold and Fishell, 2005). To examine expression of Cre protein in these mice, we stained embryonic and postnatal tissues with anti-Cre antibodies (Supp Fig. 1). Consistent with previous studies (Machold and Fishell, 2005; Wang et al., 2005), we found that the Cre transgene was first expressed by rhombic lip-derived cells that are destined to leave the cerebellum and give rise to neurons of the deep cerebellar nuclei (DCN) and brainstem (Supp. Fig 1A) (Machold and Fishell, 2005). By embryonic day 14.5 (E14.5), Cre was expressed by GNPs in the EGL (Supp. Figs. 1B–D). Cre expression persisted in the EGL for the first 2–3 weeks after birth (Supp. Fig. 1E); by adulthood, when all GNPs had differentiated into granule neurons and migrated into the internal granule layer (IGL), Cre expression was no longer detectable in the cerebellum (Supp. Fig 1F).

To determine whether Cre activity correlated with Cre protein expression, we crossed Math1-Cre mice with ROSA26 reporter (R26R) mice expressing green fluorescent protein (GFP) preceded by a loxP-flanked stop sequence (Mao et al., 2001). As shown in Figure 1A, neonatal Math1-Cre/R26R-GFP mice expressed high levels of GFP in the cerebellum. Analysis of postnatal cerebellar sections (Figure 1B) revealed GFP expression only in proliferating GNPs in the outer EGL (see Ki67+ cells in Figure 1C) and in post-mitotic granule cells in the inner

EGL and IGL (NeuN+ cells in Figure 1D). GFP could also be detected in rhombic lip-derived cells that had left the cerebellum and settled in the DCN and brain stem (Supp. Fig. 2). No GFP was seen in other cell types in the cerebellar cortex, including Purkinje neurons, basket and stellate neurons, Bergmann glia and oligodendrocytes (Figure 1E–H). By postnatal day 21 (P21), greater than 95% of NeuN positive cells expressed GFP (Supp. Fig 3A), indicating that the majority of granule cells had been exposed to Cre during development. Thus, Math1-Cre mice allow deletion of loxP-flanked genes in GNPs.

To test the effects of loss of *ptc* on GNPs, we isolated cells from the cerebellum of neonatal $Ptc^{C/C}$ mice, infected them with Cre-encoding retroviruses and analyzed expression of *ptc* and hedgehog target genes by RT-PCR. As shown in Figure 1I, cells infected with Cre viruses showed no detectable *ptc* expression. Since Ptc is a negative regulator of the hedgehog pathway (Goodrich et al., 1996), its loss should result in Shh pathway activation. Consistent with this, Cre retrovirus-mediated deletion of *ptc* resulted in increased expression of *gli1*, *cyclin D1* and *N-myc*, all previously identified as Shh target genes in GNPs (Kenney et al., 2003; Oliver et al., 2003) (Figure 1J). Finally, Shh pathway activation has been demonstrated to promote proliferation of GNPs (Wechsler-Reya and Scott, 1999); Figure 1K shows that cells infected with Cre viruses show extensive proliferation compared to cells infected with control viruses. Thus, $Ptc^{C/C}$ mice allow deletion of *ptc* and activation of the Shh pathway in GNPs.

Deletion of *ptc* in GNPs promotes proliferation but does not prevent differentiation

We next tested the effects of GNP-specific *ptc* deletion *in vivo*, by crossing $Ptc^{C/C}$ mice with Math1-Cre mice. The efficiency of *ptc* deletion in these mice was examined by laser-capturing EGL cells from Math1-Cre/$Ptc^{C/C}$ cerebella and analyzing their DNA by quantitative PCR; this analysis revealed a >90% reduction in *ptc* compared to EGL from wild-type (WT) mice (Supp Fig. 3C–D). We then examined the structure of the cerebellum in these animals at various stages of development. At E15, Math1-Cre/$Ptc^{C/C}$ mice were indistinguishable from WT littermates, and showed no significant changes in cerebellar architecture (data not shown). However, after birth (P1–P8) Math1-Cre/$Ptc^{C/C}$ animals exhibited a dramatic thickening of the EGL (Figure 2E–F) compared to WT littermates (Figure 2A–B). By P21, all GNPs in WT mice had differentiated and migrated into the IGL, and there was no EGL remaining (Figure 2D). At this stage, the cerebellum of Math1-Cre/$Ptc^{C/C}$ mice was significantly larger than that of WT littermates (Figure 2C,G), and still contained a thick EGL (Figure 2H). These data indicate that deletion of *ptc* in GNPs leads to severe cerebellar hyperplasia.

Animals with defects in granule cell development often display ataxia or other behavioral abnormalities (Hamre and Goldowitz, 1997; Surmeier et al., 1996). However, at 4–6 weeks of age most Math1-Cre/$Ptc^{C/C}$ mice displayed normal behavior, suggesting that at least some normal granule neurons were generated in these animals. To determine whether this was the case, we analyzed the cerebellum of Math1-Cre/$Ptc^{C/C}$ mice at 6-weeks. In contrast to the cerebellum of a WT mouse (Figure 3A, D), the Math1-Cre/$Ptc^{C/C}$ cerebellum still contained a thick layer of proliferating GNPs on its surface (Figure 3B, E). However, beneath this proliferative zone the normal organization of the cerebellum was maintained, with a distinct Purkinje cell layer surrounding a layer of mature granule neurons that expressed normal differentiation markers (Figure 3E and Supp. Fig. 4). Deletion of *ptc* in mature granule cells was confirmed by RT-PCR analysis after laser-capture microdissection (Figure 3G–I). Some regions of the Math1-Cre/$Ptc^{C/C}$ cerebellum were more disrupted, showing a nodular structure rather than discrete layers of cells (Figure 3C, F). However, even in these regions there was a remarkable conservation of granule cell organization and differentiation, with each nodule containing a core of proliferating GNPs surrounded by a molecular layer, a Purkinje cell layer and a ring of differentiated granule cells that resembled an IGL (Figure 3F and Supp. Fig. 4B).

These observations suggest that loss of *ptc* in GNPs results in prolonged proliferation, but that many *ptc*-deficient cells are still able to exit the cell cycle and differentiate into mature neurons.

Deletion of *ptc* in GNPs results in medulloblastoma

Although Math1-Cre/Ptc$^{C/C}$ mice were asymptomatic in early adulthood, by 8 weeks of age many animals began to display signs of illness, including domed head, hunched back, abnormal gait or decreased movement. By 10–11 weeks, all Math1-Cre/Ptc$^{C/C}$ mice became severely ill and had to be sacrificed (Figure 4F). Upon gross examination, the cerebellum from these animals appeared enlarged and covered with blood vessels (Figure 4A). Histological analysis revealed massive tumors that pervaded the cerebellum and obliterated the normal architecture that was present earlier in development (Figure 4B). The tumors could be propagated by transplantation into immunodeficient hosts, indicating that they represented fully transformed tumor cells (Figure 4C). These data suggest that deletion of *ptc* in Math1-expressing cells – while not sufficient to transform every cell – is sufficient to cause tumors in every mouse.

Although Math1 is specific to GNPs in the postnatal cerebellum, during embryonic development the Math1 enhancer is also expressed in progenitors that end up leaving the cerebellar cortex and migrating to the DCN and brainstem (Machold and Fishell, 2005; Wang et al., 2005) and Supp. Fig. 2). To determine whether the tumors in Math1-Cre/Ptc$^{C/C}$ mice could have originated from these progenitors, we crossed Ptc$^{C/C}$ mice with Math1-CreER transgenic mice (Machold and Fishell, 2005), which express a Cre recombinase-estrogen receptor fusion protein that can be activated by tamoxifen. When Math1-CreER/Ptc$^{C/C}$ mice were treated with tamoxifen at E10.5 – a stage when Math1 is only expressed by DCN and brainstem progenitors -- none of the animals (0/8 mice) developed tumors (Supp. Table 1). In contrast, when mice were treated with tamoxifen at E14.5, when Math1 is expressed in GNPs, 100% of animals (7/7) developed tumors. These data suggest that tumors in Math1-Cre/Ptc$^{C/C}$ are derived from GNPs.

GNPs are present in mice until 2–3 weeks after birth. To determine whether loss of *ptc* could trigger medulloblastoma in postnatal GNPs, we treated Math1-CreER/Ptc$^{C/C}$ mice with tamoxifen at P4, and then examined mice at several time points for changes in cerebellar structure. As with embryonic deletion, postnatal deletion of *ptc* resulted in increased GNP proliferation and expansion of the EGL by P21 (Supp Fig 5A). GNP proliferation persisted into adulthood, but the majority of *ptc*-deficient GNPs differentiated and migrated into the IGL, leaving only discrete foci of proliferating cells on the surface of the cerebellum (Supp Fig 5B). By 12 weeks of age some Math1-CreER/Ptc$^{C/C}$ animals began to exhibit symptoms of intracranial pressure, and by 19 weeks, all of these mice developed cerebellar tumors (Figure 4D–F). Tumors were also observed in mice treated with tamoxifen at P8 and P10, but not in animals treated at P12 or later (Supp. Table 1). These data indicate that both embryonic and postnatal GNPs can serve as cells of origin for medulloblastoma.

GFAP-Cre/Ptc$^{C/C}$ mice allow deletion of *ptc* in neural stem cells

Having observed that deletion of *ptc* in GNPs could cause medulloblastoma, we wondered whether deletion in NSCs would have the same effect. On one hand, since NSCs give rise to GNPs, loss of *ptc* in these cells might also be expected to result in medulloblastoma. On the other hand, NSCs can also give rise to other types of neurons and glia, so loss of *ptc* in these cells could potentially lead to other tumor types, such as astrocytoma or oligodendroglioma. To delete *ptc* in NSCs, we used GFAP-Cre mice, in which expression of Cre is controlled by the human glial fibrillary acidic protein promoter (Zhuo et al., 2001). Whereas the Math1 enhancer drives expression in progenitors after they have left the ventricular zone (VZ) and committed to the granule cell lineage (or destined for the DCN or brainstem), the GFAP promoter turns on prior to lineage commitment, in VZ progenitors that give rise to granule

neurons as well as most other types of neurons and glia in the cerebellar cortex (Casper and McCarthy, 2006; Zhuo et al., 2001).

To confirm the specificity of the GFAP-Cre transgene, we stained sections from GFAP-Cre mice with anti-Cre antibodies at various stages of development and examined expression of GFP in GFAP-Cre/R26R-GFP reporter mice. These studies revealed Cre protein expression predominantly in the VZ and in astroglial cells within the cerebellar parenchyma (Figure 5A); no Cre expression was observed in the EGL or in cells expressing Math1 (Supp. Fig. 1G–L, Supp. Fig. 6). Nonetheless, analysis of GFP expression in GFAP-Cre/R26R-GFP mice indicated that Cre-expressing cells gave rise to granule neurons as well as basket and stellate neurons, Bergmann glia and oligodendrocytes (Figure 5B–F, Supp. Fig. 3B), suggesting that the GFAP+ population included multipotent stem cells. Consistent with previous reports (Spassky et al., 2008; Zhuo et al., 2001), no labeling of Purkinje cells was observed, suggesting that these cells arise from a distinct pool of (GFAP-negative) NSCs or are generated at a stage of development prior to expression of the GFAP-Cre promoter (Hashimoto and Mikoshiba, 2003).

To confirm that the GFAP promoter is expressed in stem cells, we also isolated GFP+ cells from E14.5 GFAP-GFP cerebella (Zhuo et al., 1997) and tested their ability to form neurospheres. FACS-sorted GFAP-GFP+ cells generated neurospheres when cultured at clonal density in the presence of growth factors, and individual clones were able to differentiate into neurons, astrocytes and oligodendrocytes when growth factors were withdrawn (Supp. Fig. 7). Neurospheres also formed from GFAP-GFP-negative cells (albeit with 10-fold lower efficiency), suggesting that a subpopulation of embryonic cerebellar stem cells does not express GFAP. These studies indicate that GFAP is expressed in the majority of NSCs in the embryonic cerebellum and that its promoter can be used to target cells at an earlier stage of differentiation than the Math1-Cre mouse.

Deletion of *ptc* in stem cells results in medulloblastoma

To examine the consequences of *ptc* deletion in GFAP-expressing cells, we crossed the GFAP-Cre mice with $Ptc^{C/C}$ mice and analyzed progeny during embryonic and postnatal development. Between E14.5-E16.5, GFAP-Cre/$Ptc^{C/C}$ mice showed expansion of the VZ, accompanied by increased proliferation and increased expression of group B1 Sox proteins, markers of multipotent stem cells (Figure 6A–D) (Pevny and Placzek, 2005; Tanaka et al., 2004). Consistent with this, cerebellar cells from GFAP-Cre/$Ptc^{C/C}$ mice generated an increased number of neurospheres compared to WT mice (Figure 6E). These neurospheres were able to differentiate into neurons, astrocytes and oligodendrocytes (Supp. Fig. 8). Increased neurosphere formation was also observed in $Ptc^{C/C}$ cells infected with Cre retroviruses *in vitro* (Figure 6F). Together these data suggest that GFAP-Cre-mediated deletion of *ptc* results in increased proliferation of NSCs.

During development, NSCs give rise to astrocytes, oligodendrocytes and several types of neurons. In the GFAP-Cre/$Ptc^{C/C}$ mice, these cells should all lack *ptc*, since they arise from *ptc*-deficient NSCs. Despite this, no obvious abnormalities were seen in astrocytes, oligodendrocytes or non-granule neurons of GFAP-Cre/$Ptc^{C/C}$ mice (data not shown). In contrast, marked changes were seen in VZ-derived cells that migrated to the rhombic lip and committed to the granule lineage. GFAP-Cre/$Ptc^{C/C}$ mice exhibited a dramatic expansion of the rhombic lip and EGL at E16.5 (Figure 7A–B). After birth, when the WT cerebellum contained only 1–2 rows of GNPs on its surface, the GFAP-Cre/$Ptc^{C/C}$ cerebellum was encompassed by a thick, disorganized EGL (Figure 7C–D). Analysis of genomic *ptc* from the postnatal EGL confirmed that there was near-complete (>90%) deletion of *ptc* at this stage (Supp. Fig. 3C–D). By P14, the entire cerebellum was filled with GNP-like cells, and animals began to show symptoms of illness (Figure 7E–F). By 4 weeks, all GFAP-Cre/$Ptc^{C/C}$ mice

developed cerebellar tumors (Figure 7G–H, I). These data show that tumors can be induced by deletion of *ptc* in multipotent progenitors as well as in lineage-restricted GNPs.

Interestingly, tumors in Math1-Cre/$Ptc^{C/C}$ mice and GFAP-Cre/$Ptc^{C/C}$ mice expressed abundant and comparable levels of the GNP marker Math1 and the proliferation marker Ki67 (Figure 8A–D). In regions of differentiation, most cells expressed the neuronal differentiation markers NeuN, synaptophysin and GABRA6 (Figure 8E–F and data not shown). Few tumor cells in either strain expressed markers of neural stem cells, non-granule neurons or glia, and cells that did express these markers were almost never proliferating (Figure 8G–J). Tumor cells from GFAP-Cre/$Ptc^{C/C}$ mice and Math1-Cre/$Ptc^{C/C}$ mice also exhibited similar levels of proliferation (Figure 8K), and induced tumors with similar efficiency and latency following transplantation of $0.5–10 \times 10^5$ tumor cells into immunodeficient hosts (Figure 8L and data not shown). These observations indicate that tumors initiated in stem cells and progenitors are remarkably similar. The dramatic expansion of the EGL in neonatal GFAP-Cre/$Ptc^{C/C}$ mice and the predominant expression of GNP markers in tumors from both strains suggest that tumor formation in these animals is restricted to the granule lineage. Thus, medulloblastoma can be initiated by deletion of *ptc* in multipotent stem cells or lineage restricted progenitors, but the oncogenic effects of Shh signaling are only manifest once cells have committed to the granule lineage.

DISCUSSION

The origin of medulloblastoma has been the subject of controversy for many years (Eberhart, 2007; Read et al., 2006). Although some investigators have speculated that these tumors arise from GNPs, the evidence has been largely circumstantial: the morphology of tumor cells, the location of these cells on the surface of the cerebellum (where GNPs develop) and the expression of GNP-associated markers. The fact that Shh is mitogenic for GNPs (Wechsler-Reya and Scott, 1999) and the observation that medulloblastomas in $ptc^{+/-}$ mice resemble GNPs (Goodrich et al., 1997; Oliver et al., 2005) have suggested that *ptc*-associated tumors in particular might be derived from these cells. However, the recent observations that Shh is required for stem cell growth and maintenance (Ahn and Joyner, 2005; Balordi and Fishell, 2007) and that medulloblastomas often express stem cell markers (Hemmati et al., 2003; Singh et al., 2003) have cast doubt on this view. By deleting *ptc* in GNPs and in stem cells, we provide direct evidence that each of these cells can serve as a cell of origin for Shh pathway-associated medulloblastoma.

Tumorigenesis is thought to depend on a capacity for long-term self-renewal. During normal development, GNPs do not exhibit this capacity: they proliferate for 2–3 weeks after birth and then exit the cell cycle and undergo terminal differentiation. The fact that GNPs in Math1-Cre/$Ptc^{C/C}$ mice continue to proliferate into adulthood (and continue to divide following transplantation) suggests that loss of *ptc* can increase the self-renewal capacity of these cells. Thus, while neural stem cells – which are thought to have an intrinsic capacity for long-term self-renewal – might represent a good target for oncogenic transformation, restricted progenitors can also become transformed if, through mutation, they acquire the capacity for long-term self-renewal. The ability of oncogenic mutations to increase the self-renewal capacity of lineage-restricted progenitors has also been demonstrated in the hematopoietic system (Cozzio et al., 2003; Krivtsov et al., 2006).

Our studies show that deletion of *ptc* in GNPs promotes a dramatic increase in proliferation of these cells and results in tumors in all mice. However, it is notable that in Math1-Cre/$Ptc^{C/C}$ and Math1-CreER-$Ptc^{C/C}$ mice, many GNPs are able to differentiate despite loss of *ptc*, and only a subset of cells continues to proliferate and forms tumors. One explanation for this is that full transformation of GNPs requires changes besides loss of *ptc*, and these changes only occur

in a subset of GNPs. This notion is supported by our studies of conventional $ptc^{+/-}$ mice (Oliver et al., 2005), which demonstrated that loss of *ptc* results in pre-neoplastic lesions, but that most of these lesions do not go on to become tumors. Expression profiling of GNPs, pre-neoplastic cells and tumor cells suggested that altered expression of genes involved in cell migration, differentiation or apoptosis might be necessary for complete transformation.

In addition to GNPs, tumors can also be initiated by deletion of *ptc* in NSCs. Loss of *ptc* in NSCs initially results in expansion of the VZ and increased numbers of stem cells. Our demonstration that *ptc* deletion causes proliferation of cerebellar stem cells is consistent with previous reports showing a role for Shh in stem cell renewal in other parts of the CNS (Ahn and Joyner, 2005; Balordi and Fishell, 2007). Importantly, while *ptc*-deficient NSCs exhibit increased proliferation, they remain capable of differentiating into astrocytes, oligodendrocytes and neurons. Indeed, the most dramatic consequences of *ptc* deletion occur once cells leave the VZ and commit to the granule cell lineage. GNPs in GFAP-Cre/$Ptc^{C/C}$ mice undergo rapid expansion, encompass the cerebellum at early postnatal stages and appear to give rise to medulloblastomas in these mice. Support for this notion comes from the fact that the majority of cells in GFAP-Cre/$Ptc^{C/C}$ tumors (like those in Math1-Cre/$Ptc^{C/C}$ tumors) express GNP markers rather than NSC markers. Moreover, the differentiated cells present within these tumors predominantly express markers of post-mitotic granule neurons (NeuN, GABRA6) rather than non-granule neurons, astrocytes or oligodendrocytes, as would be expected if tumors retained characteristics of multipotent stem cells. The fact that deletion of *ptc* in NSCs does not lead to other tumor types (e.g. astrocytomas, oligodendrogliomas or even medulloblastomas with non-GNP characteristics) is remarkable, and suggests that the granule lineage may be exquisitely sensitive to the oncogenic effects of hedgehog signaling. Alternatively, it is possible that additional genetic or epigenetic events (besides loss of *ptc*) are needed for tumor formation, and that these are most likely to occur during the rapid expansion of GNPs in the EGL.

While our data suggest that deletion of *ptc* in GFAP-expressing NSCs does not result in glial tumors, this does not mean that Shh signaling does not play any role in initiation or maintenance of such tumors. For example, it is possible that activation of the hedgehog pathway in distinct progenitors, or in combination with additional oncogenic lesions, might result in formation of astrocytomas or oligodendrogliomas. Moreover, recent studies have suggested that the Shh pathway is active in human glioma and in mouse models of the disease (Becher et al., 2008; Clement et al., 2007; Ehtesham et al., 2007), and that treatment with Shh pathway inhibitors can suppress the growth of glioma cell lines and xenografts (Bar et al., 2007; Clement et al., 2007). These data raise the possibility that Shh signaling, even if it is not involved in tumor initiation, might contribute to tumor growth or maintenance. Further studies of Shh pathway antagonists in transgenic and xenograft models of glioma will be required to determine the importance of this pathway as a therapeutic target.

In the discussion above, we refer to the tumors in GFAP-Cre/$Ptc^{C/C}$ mice as being “initiated” in NSCs. Since these tumors do not manifest until cells have committed to the granule lineage, it is reasonable to ask whether they should be more aptly considered to be initiated in GNPs. In this context, we believe it is important to draw a distinction between tumor initiation and transformation. We consider tumor initiation to be the stage at which the first oncogenic mutation occurs, even if this mutation is not sufficient to fully transform the cell. In contrast, we view transformation as the stage at which cells have accumulated all the oncogenic mutations that they need to form tumors. With this framework in mind, we believe it is appropriate to refer to tumors in GFAP-Cre/$Ptc^{C/C}$ mice as initiated in stem cells, and to consider NSCs as the “cells of origin” for these tumors.

In comparing tumors in GFAP-Cre/Ptc$^{C/C}$ and Math1-Cre/Ptc$^{C/C}$ mice, the only marked difference we observed was in tumor latency: GFAP-Cre/Ptc$^{C/C}$ mice developed tumors between 3–4 weeks of age, whereas Math1-Cre/Ptc$^{C/C}$ mice developed tumors between 8–12 weeks. One possible explanation for the rapid expansion of tumors in GFAP-Cre/Ptc$^{C/C}$ mice is that deletion of *ptc* in these animals is more efficient than in Math1-Cre/Ptc$^{C/C}$ mice, and as a result, there are more *ptc*-deficient GNPs to serve as a source for the tumors. However, our analysis suggests that Cre activity (based on induction of GFP in R26R reporter mice) and *ptc* deletion efficiency (based on analysis of genomic *ptc* levels) are very similar between the two strains. Another possible explanation for the difference in latency is that GFAP-Cre/Ptc$^{C/C}$ tumor cells have an increased rate of proliferation or a decreased rate of apoptosis, and as a result give rise to more rapidly growing tumors. However, comparison of thymidine incorporation, cell cycle analysis, caspase activation and even gene expression has not revealed any significant differences in these parameters between GFAP-Cre/Ptc$^{C/C}$ and Math1-Cre/Ptc$^{C/C}$ tumor cells (Figure 8 and unpublished observations). Moreover, transplantation of equal numbers of GFAP-Cre/Ptc$^{C/C}$ and Math1-Cre/Ptc$^{C/C}$ tumor cells into immunocompromised mice results in similar tumor latency in recipients. Thus, intrinsic differences between GFAP-Cre/Ptc$^{C/C}$ and Math1-Cre/Ptc$^{C/C}$ tumor cells are also not likely to account for the differences in age of tumor onset.

Instead, the differences in tumor latency are most likely a consequence of the stage at which *ptc* deletion occurs. Deletion of *ptc* in the VZ (using GFAP-Cre) leads to an early expansion of the stem cell pool. A larger stem cell pool leads, in turn, to a significant increase in the starting number of GNPs, which then continue to expand and ultimately contribute to tumor bulk. Since animals develop symptoms when tumors reach a critical mass, having a larger pool of *ptc*-deficient GNPs at the outset allows GFAP-Cre/Ptc$^{C/C}$ mice to reach this stage much more quickly than Math1-Cre/Ptc$^{C/C}$ mice. This model may also explain the shorter latency of tumors in Math1-Cre/Ptc$^{C/C}$ mice compared to Math1-CreER/Ptc$^{C/C}$ mice that are exposed to tamoxifen postnatally: whereas embryonic deletion of *ptc* targets all GNPs, postnatal deletion targets only the subset of GNPs that have not yet differentiated. As a result, it takes GNPs in postnatally targeted animals longer to reach critical mass. The same may be true for tumors in other tissues: the earlier in a given lineage an oncogenic mutation occurs, the more opportunity there is for expansion of cells bearing this mutation, and the more dramatic the consequences for the animal.

These observations may have particular significance for human medulloblastoma. Although medulloblastoma can occur in children as well as adults, patients who develop tumors at a very young age (< 3 years) have a high risk for treatment failure and relapse, while those who develop the disease when they are older tend to have a more favorable outcome (Kalifa and Grill, 2005). One reason for this may be that radiation therapy, which is commonly used in older patients, is withheld from young children because it is considered to be too damaging for the developing brain. Thus, tumors in young children may grow faster because they are treated less aggressively. However, our findings suggest that the cell in which the tumor was initiated may also contribute to the age of onset and the difference in prognosis: tumors that occur in young children may arise from mutations in multipotent stem cells whereas those in older children may originate from more differentiated progenitors. In the former case, as in our GFAP-Cre/Ptc$^{C/C}$ mice, expansion of stem cells and increased production of GNPs may contribute to more rapid tumor growth and earlier onset of symptoms.

Identifying the cell of origin for medulloblastoma may also have important implications for therapy. Recent studies have shown that many brain tumors contain NSC-like cells, and have suggested that these cells are important for tumor propagation (Hemmati et al., 2003; Singh et al., 2004). In light of this, many investigators have begun to develop targeted therapies to eradicate such cells. Our studies demonstrate that not all brain tumors are derived from cells

with a stem cell phenotype. In particular, we show that Shh pathway-associated medulloblastomas may be initiated in either progenitors or stem cells, and ultimately adopt a phenotype that resembles GNPs rather than NSCs. Whether the same is true for other subtypes of medulloblastoma remains to be investigated. Determining whether a tumor is derived from lineage-restricted progenitors or stem cells, finding markers specific for these cells and identifying signals that control their growth and differentiation may be important prerequisites for effective therapy.

EXPERIMENTAL PROCEDURES

Mice

$Ptc^{C/C}$ mice and Math1-Cre-ER mice have been described previously (Ellis et al., 2003; Machold and Fishell, 2005). GFAP-GFP (Zhuo et al., 1997), GFAP-Cre mice (Zhuo et al., 2001) and R26R-GFP reporter mice (Mao et al., 2001) were from Jackson Labs (Bar Harbor, ME). SCID-beige mice were from Charles River (Wilmington, MA). Animals were maintained in the Cancer Center Isolation Facility at Duke University, and all experiments were performed in accordance with procedures approved by the Duke University Animal Care and Use Committee.

Histology and immunohistochemistry

For histological analysis, animals were perfused with PBS followed by 4% paraformaldehyde (PFA). Cerebella were removed, fixed in 4% PFA overnight, transferred to 70% ethanol and paraffin-embedded. 5-μM sections were stained with hematoxylin and eosin (H&E, Sigma, St. Louis, MO) or with anti-BrdU or anti-Group B1 Sox antibodies (Tanaka et al., 2004).

For immunohistochemistry, cerebella from PFA-perfused animals were fixed overnight in 4% PFA, cryoprotected in 30% sucrose, frozen in Tissue Tek-OCT (Sakura Finetek, Torrance, CA) and cut into 10–12um saggital sections. Sections were blocked and permeabilized for 2 hours with PBS containing 0.1% Triton X-100 and 1% normal goat serum, stained with primary antibodies overnight at 4°C, and incubated with secondary antibodies for 2h at room temperature. Sections were counterstained with DAPI and mounted with Fluoromount G (Southern Biotechnology, Birmingham, AL) before being visualized using a Nikon TE-200 microscope. Antibodies used for immunostaining are listed in Supplementary Methods.

Cell isolation and Proliferation assays

Cerebella from P6 mice were digested with 10U/ml papain (Worthington, Lakewood, NJ), 200ug/ml L-cysteine and 250 U/ml DNase (Sigma), triturated to obtain a single cell suspension and then centrifuged through a 35%–65% Percoll gradient (Sigma). Cells from the 35–65% interface were suspended in NB-B27 (Neurobasal with 1mM sodium pyruvate, 2mM L-glutamine, Pen/Strep and B27 supplement, all from Invitrogen) and transferred to Poly-D-lysine-coated 96-well plates at a density of 2×10^5 cells per well. After 48h, cells were pulsed with methyl-^{3}H thymidine (Amersham/GE Healthcare, Piscataway, NJ) and cultured for an additional 16–18 h. Cells were harvested onto filters using a Mach IIIM Manual Harvester 96 (Tomtec, Hamden, CT) and incorporated radioactivity was quantified by liquid scintillation spectrophotometry on a Wallac MicroBeta scintillation counter (Perkin Elmer, Wellesley, MA).

Laser capture microdissection and real-time RT-PCR

Cerebella were removed immediately and frozen in OCT. 5-μM sagittal sections were mounted onto glass slides, fixed in 75% ethanol for 30 sec, and stained with Cresyl Violet (Ambion, Austin, TX). After 5 min of air-drying, microdissection was carried out using a PixCell IIe

LCM system (Arcturus Bioscience, Sunnyvale, CA). RNA was extracted from LCM caps using an RNA isolation kit (Arcturus). For real time RT-PCR, first strand cDNA was synthesized from equal amounts of RNA (0.1–1 μg) using Superscript III Reverse Transcriptase (Invitrogen). Triplicate reactions were prepared using a 25-μl mixture containing iQ SYBR Green Supermix (Biorad, Hercules, CA). Real-time quantification was performed on a BIO-RAD iCycler iQ system (BioRad). Serial 10-fold dilutions of cDNA were used as references for the standard curve. Raw data were normalized based on expression of actin. Primers used for *gli1*, *Nmyc*, *cyclin D1* and *ptc* are listed in Supplementary Methods.

Intracranial transplantation

SCID-beige mice (6–8 weeks old) were anesthetized with a xylazine (25 mg/kg, Lloyd Laboratories, Shenandoah, IA) and ketamine (125 mg/kg, Fort Dodge Animal Health, Fort Dodge, IA), and placed in a stereotaxic apparatus (Kopf, Tujunga, CA). After exposing the skull with a scalpel, a 1 mm diameter hole was drilled in the skull over the cerebellum using an 18G needle. A cell suspension (1×10^6 cells in 5-μl NB-B27) was slowly injected into the cerebellum at a depth of 1mm, using a 5-μl Hamilton Syringe with an unbevelled 24G needle (Hamilton, Reno, NV). After injection, the incision was sutured using catgut sutures (Johnson & Johnson, Piscataway, NJ).

Tamoxifen treatment

Tamoxifen (T-5648, Sigma) was prepared as a 20 mg/ml stock solution in corn oil (Sigma). Tamoxifen was administered by oral gavage using 24-G gavaging needles (Fine Science Tools, Foster City, CA). Tamoxifen doses were: 0.6 mg/30 μl at P4, 1 mg/50 μl at P8, 1.4 mg/70 μl at P10, 1.6 mg/80 μl at P12 and 4.0 mg/200μl for treatment of pregnant females.

Neurosphere cultures

To generate primary neurospheres, cells from E14.5 embryonic cerebella were plated at 2×10^5 cells/ml in NSC proliferation medium (NeuroCult Basal Medium with Proliferation Supplement, Stem Cell Technologies, Seattle, WA) plus 10 ng/ml basic fibroblast growth factor and 20 ng/ml epidermal growth factor (Peprotech, Rocky Hill, NJ). Neurospheres were counted or harvested for immunostaining after 7 days in culture. To passage, neurospheres were mechanically dissociated and re-plated in fresh proliferation medium at 2×10^3 cells/ml. For differentiation, neurospheres were plated on Poly-D-lysine coated coverslips (BD Biosciences) in NSC differentiation medium (NeuroCult Basal Medium with Differentiation Supplement). Seven days after plating, cultures were fixed with 4% PFA for immunostaining.

Supplementary Material

Refer to Web version on PubMed Central for supplementary material.

Acknowledgements

The authors thank Susan Su, Pate Skene and the NIH Neuroscience Microarray Consortium for help with laser capture and microarray analysis, Simon Lin at Northwestern University for assistance with bioinformatics, Beth Harvat and Mike Cook for flow cytometry, and Jack Dutton, Mark Johnson and Zhen Zhao for assistance with animal colony maintenance. Tammy Ellis is a John Trivett Senior Research Fellow. This work was supported by funds from the National Health and Medical Research Council of Australia (B.J.W.), the ARC Special Research Centre for Functional and Applied Genomics (B.J.W.), Queensland Cancer Fund (B.J.W.), the Hope Street Kids Foundation (Z.J.Y.), the Kislak-Sussman Fund (R.W.R.), the Children's Brain Tumor Foundation (R.W.R), the Pediatric Brain Tumor Foundation (R.W.R.), the McDonnell Foundation (R.W.R.) and NINDS grant number NS052323-01 (R.W.R.).

Abbreviations

GNP granule neuron precursor

NSC neural stem cell

DCN deep cerebellar nuclei

Shh Sonic hedgehog

EGL external germinal layer

IGL internal granule layer

VZ ventricular zone

References

Adolphe C, Hetherington R, Ellis T, Wainwright B. Patched1 functions as a gatekeeper by promoting cell cycle progression. Cancer research 2006;66:2081–2088. [PubMed: 16489008]

Ahn S, Joyner AL. In vivo analysis of quiescent adult neural stem cells responding to Sonic hedgehog. Nature 2005;437:894–897. [PubMed: 16208373]

Balordi F, Fishell G. Hedgehog signaling in the subventricular zone is required for both the maintenance of stem cells and the migration of newborn neurons. J Neurosci 2007;27:5936–5947. [PubMed: 17537964]

Bar EE, Chaudhry A, Lin A, Fan X, Schreck K, Matsui W, Piccirillo S, Vescovi AL, DiMeco F, Olivi A, Eberhart CG. Cyclopamine-mediated hedgehog pathway inhibition depletes stem-like cancer cells in glioblastoma. Stem Cells 2007;25:2524–2533. [PubMed: 17628016]

Becher OJ, Hambardzumyan D, Fomchenko EI, Momota H, Mainwaring L, Bleau AM, Katz AM, Edgar M, Kenney AM, Cordon-Cardo C, et al. Gli activity correlates with tumor grade in platelet-derived growth factor-induced gliomas. Cancer research 2008;68:2241–2249. [PubMed: 18381430]

Buhren J, Christoph AH, Buslei R, Albrecht S, Wiestler OD, Pietsch T. Expression of the neurotrophin receptor p75NTR in medulloblastomas is correlated with distinct histological and clinical features: evidence for a medulloblastoma subtype derived from the external granule cell layer. Journal of neuropathology and experimental neurology 2000;59:229–240. [PubMed: 10744061]

Casper KB, McCarthy KD. GFAP-positive progenitor cells produce neurons and oligodendrocytes throughout the CNS. Mol Cell Neurosci 2006;31:676–684. [PubMed: 16458536]

Clement V, Sanchez P, de Tribolet N, Radovanovic I, Ruiz i Altaba A. HEDGEHOG-GLI1 signaling regulates human glioma growth, cancer stem cell self-renewal, and tumorigenicity. Curr Biol 2007;17:165–172. [PubMed: 17196391]

Cozzio A, Passegue E, Ayton PM, Karsunky H, Cleary ML, Weissman IL. Similar MLL-associated leukemias arising from self-renewing stem cells and short-lived myeloid progenitors. Genes & development 2003;17:3029–3035. [PubMed: 14701873]

Eberhart CG. In search of the medulloblast: neural stem cells and embryonal brain tumors. Neurosurg Clin N Am 2007;18:59–69. viii–ix. [PubMed: 17244554]

Ehtesham M, Sarangi A, Valadez JG, Chanthaphaychith S, Becher MW, Abel TW, Thompson RC, Cooper MK. Ligand-dependent activation of the hedgehog pathway in glioma progenitor cells. Oncogene 2007;26:5752–5761. [PubMed: 17353902]

Ellis T, Smyth I, Riley E, Graham S, Elliot K, Narang M, Kay GF, Wicking C, Wainwright B. Patched 1 conditional null allele in mice. Genesis 2003;36:158–161. [PubMed: 12872247]

Ellison D. Classifying the medulloblastoma: insights from morphology and molecular genetics. Neuropathol Appl Neurobiol 2002;28:257–282. [PubMed: 12175339]

Gilbertson RJ, Ellison DW. The origins of medulloblastoma subtypes. Annual review of pathology 2008;3:341–365.

Goodrich LV, Johnson RL, Milenkovic L, McMahon JA, Scott MP. Conservation of the hedgehog/patched signaling pathway from flies to mice: induction of a mouse patched gene by Hedgehog. Genes & development 1996;10:301–312. [PubMed: 8595881]

Goodrich LV, Milenkovic L, Higgins KM, Scott MP. Altered neural cell fates and medulloblastoma in mouse *patched* mutants. Science (New York, NY 1997;277:1109–1113.

Hahn H, Wicking C, Zaphiropoulous PG, Gailani MR, Shanley S, Chidambaram A, Vorechovsky I, Holmberg E, Unden AB, Gillies S, et al. Mutations of the human homolog of Drosophila patched in the nevoid basal cell carcinoma syndrome. Cell 1996;85:841–851. [PubMed: 8681379]

Hahn H, Wojnowski L, Specht K, Kappler R, Calzada-Wack J, Potter D, Zimmer A, Muller U, Samson E, Quintanilla-Martinez L. Patched target Igf2 is indispensable for the formation of medulloblastoma and rhabdomyosarcoma. The Journal of biological chemistry 2000;275:28341–28344. [PubMed: 10884376]

Hamre KM, Goldowitz D. meander tail acts intrinsic to granule cell precursors to disrupt cerebellar development: analysis of meander tail chimeric mice. Development 1997;124:4201–4212. [PubMed: 9334269]

Hashimoto M, Mikoshiba K. Mediolateral compartmentalization of the cerebellum is determined on the “birth date” of Purkinje cells. J Neurosci 2003;23:11342–11351. [PubMed: 14672998]

Heikens J, Michiels EM, Behrendt H, Endert E, Bakker PJ, Fliers E. Long-term neuro-endocrine sequelae after treatment for childhood medulloblastoma. Eur J Cancer 1998;34:1592–1597. [PubMed: 9893634]

Hemmati HD, Nakano I, Lazareff JA, Masterman-Smith M, Geschwind DH, Bronner-Fraser M, Kornblum HI. Cancerous stem cells can arise from pediatric brain tumors. Proceedings of the National Academy of Sciences of the United States of America 2003;100:15178–15183. [PubMed: 14645703]

Johnson RL, Rothman AL, Xie J, Goodrich LV, Bare JW, Bonifas JM, Quinn AG, Myers RM, Cox DR, Epstein EH Jr, Scott MP. Human homolog of patched, a candidate gene for the basal cell nevus syndrome. Science (New York, NY 1996;272:1668–1671.

Kalifa C, Grill J. The therapy of infantile malignant brain tumors: current status? J Neurooncol 2005;75:279–285. [PubMed: 16195802]

Kenney AM, Cole MD, Rowitch DH. Nmyc upregulation by sonic hedgehog signaling promotes proliferation in developing cerebellar granule neuron precursors. Development 2003;130:15–28. [PubMed: 12441288]

Krivtsov AV, Twomey D, Feng Z, Stubbs MC, Wang Y, Faber J, Levine JE, Wang J, Hahn WC, Gilliland DG, et al. Transformation from committed progenitor to leukaemia stem cell initiated by MLL-AF9. Nature 2006;442:818–822. [PubMed: 16862118]

Machold R, Fishell G. Math1 is expressed in temporally discrete pools of cerebellar rhombic-lip neural progenitors. Neuron 2005;48:17–24. [PubMed: 16202705]

Mao X, Fujiwara Y, Chapdelaine A, Yang H, Orkin SH. Activation of EGFP expression by Cre-mediated excision in a new ROSA26 reporter mouse strain. Blood 2001;97:324–326. [PubMed: 11133778]

Mulhern RK, Palmer SL, Merchant TE, Wallace D, Kocak M, Brouwers P, Krull K, Chintagumpala M, Stargatt R, Ashley DM, et al. Neurocognitive consequences of risk-adapted therapy for childhood medulloblastoma. J Clin Oncol 2005;23:5511–5519. [PubMed: 16110011]

Oliver TG, Grasfeder LL, Carroll AL, Kaiser C, Gillingham CL, Lin SM, Wickramasinghe R, Scott MP, Wechsler-Reya RJ. Transcriptional profiling of the Sonic hedgehog response: a critical role for N-myc in proliferation of neuronal precursors. Proceedings of the National Academy of Sciences of the United States of America 2003;100:7331–7336. [PubMed: 12777630]

Oliver TG, Read TA, Kessler JD, Mehmeti A, Wells JF, Huynh TT, Lin SM, Wechsler-Reya RJ. Loss of patched and disruption of granule cell development in a pre-neoplastic stage of medulloblastoma. Development 2005;132:2425–2439. [PubMed: 15843415]

Packer RJ, Cogen P, Vezina G, Rorke LB. Medulloblastoma: clinical and biologic aspects. Neuro-oncol 1999;1:232–250. [PubMed: 11550316]

Pevny L, Placzek M. SOX genes and neural progenitor identity. Curr Opin Neurobiol 2005;15:7–13. [PubMed: 15721738]

Pomeroy SL, Sutton ME, Goumnerova LC, Segal RA. Neurotrophins in cerebellar granule cell development and medulloblastoma. J Neurooncol 1997;35:347–352. [PubMed: 9440031]

Raffel C, Jenkins RB, Frederick L, Hebrink D, Alderete B, Fults DW, James CD. Sporadic medulloblastomas contain PTCH mutations. Cancer research 1997;57:842–845. [PubMed: 9041183]

Read TA, Hegedus B, Wechsler-Reya R, Gutmann DH. The neurobiology of neurooncology. Ann Neurol 2006;60:3–11. [PubMed: 16802285]

Romer JT, Kimura H, Magdaleno S, Sasai K, Fuller C, Baines H, Connelly M, Stewart CF, Gould S, Rubin LL, Curran T. Suppression of the Shh pathway using a small molecule inhibitor eliminates medulloblastoma in Ptc1(+/−)p53(−/−) mice. Cancer cell 2004;6:229–240. [PubMed: 15380514]

Salsano E, Pollo B, Eoli M, Giordana MT, Finocchiaro G. Expression of MATH1, a marker of cerebellar granule cell progenitors, identifies different medulloblastoma sub-types. Neurosci Lett 2004;370:180–185. [PubMed: 15488319]

Sanchez P, Ruiz i Altaba A. In vivo inhibition of endogenous brain tumors through systemic interference of Hedgehog signaling in mice. Mech Dev 2005;122:223–230. [PubMed: 15652709]

Schuller U, Zhao Q, Godinho SA, Heine VM, Medema RH, Pellman D, Rowitch DH. Forkhead transcription factor FoxM1 regulates mitotic entry and prevents spindle defects in cerebellar granule neuron precursors. Molecular and cellular biology 2007;27:8259–8270. [PubMed: 17893320]

Singh SK, Clarke ID, Terasaki M, Bonn VE, Hawkins C, Squire J, Dirks PB. Identification of a cancer stem cell in human brain tumors. Cancer research 2003;63:5821–5828. [PubMed: 14522905]

Singh SK, Hawkins C, Clarke ID, Squire JA, Bayani J, Hide T, Henkelman RM, Cusimano MD, Dirks PB. Identification of human brain tumour initiating cells. Nature 2004;432:396–401. [PubMed: 15549107]

Spassky N, Han YG, Aguilar A, Strehl L, Besse L, Laclef C, Romaguera Ros M, Garcia-Verdugo JM, Alvarez-Buylla A. Primary cilia are required for cerebellar development and Shh-dependent expansion of progenitor pool. Developmental biology. 2008

Surmeier DJ, Mermelstein PG, Goldowitz D. The weaver mutation of GIRK2 results in a loss of inwardly rectifying K+ current in cerebellar granule cells. Proceedings of the National Academy of Sciences of the United States of America 1996;93:11191–11195. [PubMed: 8855331]

Tanaka S, Kamachi Y, Tanouchi A, Hamada H, Jing N, Kondoh H. Interplay of SOX and POU factors in regulation of the Nestin gene in neural primordial cells. Molecular and cellular biology 2004;24:8834–8846. [PubMed: 15456859]

Wang VY, Rose MF, Zoghbi HY. Math1 expression redefines the rhombic lip derivatives and reveals novel lineages within the brainstem and cerebellum. Neuron 2005;48:31–43. [PubMed: 16202707]

Wechsler-Reya RJ, Scott MP. Control of neuronal precursor proliferation in the cerebellum by Sonic Hedgehog. Neuron 1999;22:103–114. [PubMed: 10027293]

Wetmore C, Eberhart DE, Curran T. Loss of p53 but not ARF accelerates medulloblastoma in mice heterozygous for patched. Cancer research 2001;61:513–516. [PubMed: 11212243]

Yokota N, Aruga J, Takai S, Yamada K, Hamazaki M, Iwase T, Sugimura H, Mikoshiba K. Predominant expression of human zic in cerebellar granule cell lineage and medulloblastoma. Cancer research 1996;56:377–383. [PubMed: 8542595]

Zhuo L, Sun B, Zhang CL, Fine A, Chiu SY, Messing A. Live astrocytes visualized by green fluorescent protein in transgenic mice. Developmental biology 1997;187:36–42. [PubMed: 9224672]

Zhuo L, Theis M, Alvarez-Maya I, Brenner M, Willecke K, Messing A. hGFAP-cre transgenic mice for manipulation of glial and neuronal function in vivo. Genesis 2001;31:85–94. [PubMed: 11668683]

Zindy F, Uziel T, Ayrault O, Calabrese C, Valentine M, Rehg JE, Gilbertson RJ, Sherr CJ, Roussel MF. Genetic Alterations in Mouse Medulloblastomas and Generation of Tumors De novo from Primary Cerebellar Granule Neuron Precursors. Cancer research 2007;67:2676–2684. [PubMed: 17363588]

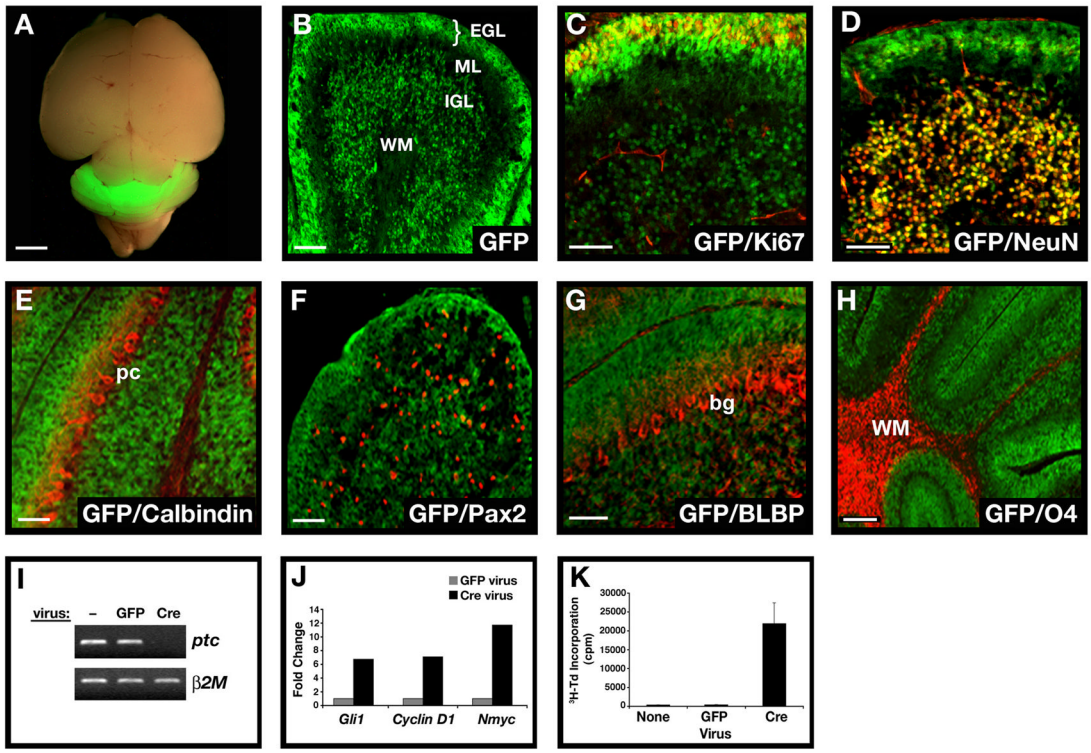

Figure 1. Conditional knockout mice allow GNP-specific deletion of *ptc* and activation of the hedgehog pathway

A. Brain from P8 Math1-Cre/R26R-GFP mouse shows Cre-induced GFP expression in the cerebellum. B. Cerebellar sections show GFP in the external and internal granule layers (EGL and IGL), but not in the molecular layer (ML) or white matter (WM). Within the EGL and IGL, GFP co-localizes with proliferating (Ki67+) GNPs and post-mitotic (NeuN+) GNPs and granule neurons (yellow staining in C and D). No GFP is detected in Calbindin+ Purkinje cells (pc, panel E), Pax2+ interneuron progenitors (F), BLBP+ Bergmann glia (bg) and astrocytes (G), or O4+ oligodendrocytes in the WM (H). I-J. GNPs from neonatal $Ptc^{C/C}$ mice were infected with no virus (−) or viruses carrying GFP or Cre-IRES-GFP. Infected (GFP+) cells were FACS-sorted and mRNA analyzed by conventional RT-PCR (I) to detect *ptc* and beta2-microglobulin (b2M), or by real-time RT-PCR (J) to detect expression of hedgehog target genes *gli1*, *cyclin D1* and *N-myc*. K. Cells infected with indicated viruses were cultured for 48h before being pulsed with tritiated thymidine (^{3}H-Td), cultured for an additional 18h, and harvested to measure thymidine incorporation. Data represent means of triplicate samples ± SEM. Scale bars: panel A, 3mm; panels B-H, 25μm.

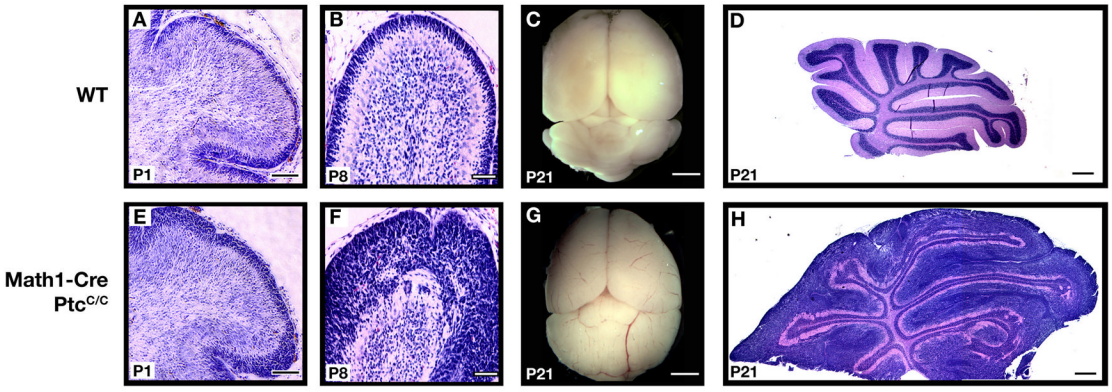

Figure 2. Deletion of *ptc* in GNPs leads to severe hyperplasia

Math1-Cre mice were crossed with $Ptc^{C/C}$ mice, and brains of WT or mutant progeny were harvested at indicated ages. Brains were fixed and photographed intact (C, G) or sectioned and stained with H&E (A, B, D, E, F, H). Note the enlargement of the cerebellum and severe hyperplasia on the surface at P8 and P21. Scale bars: 30 μm (A, B, E and F); 2.5mm (C and G); 400 μm (D and H).

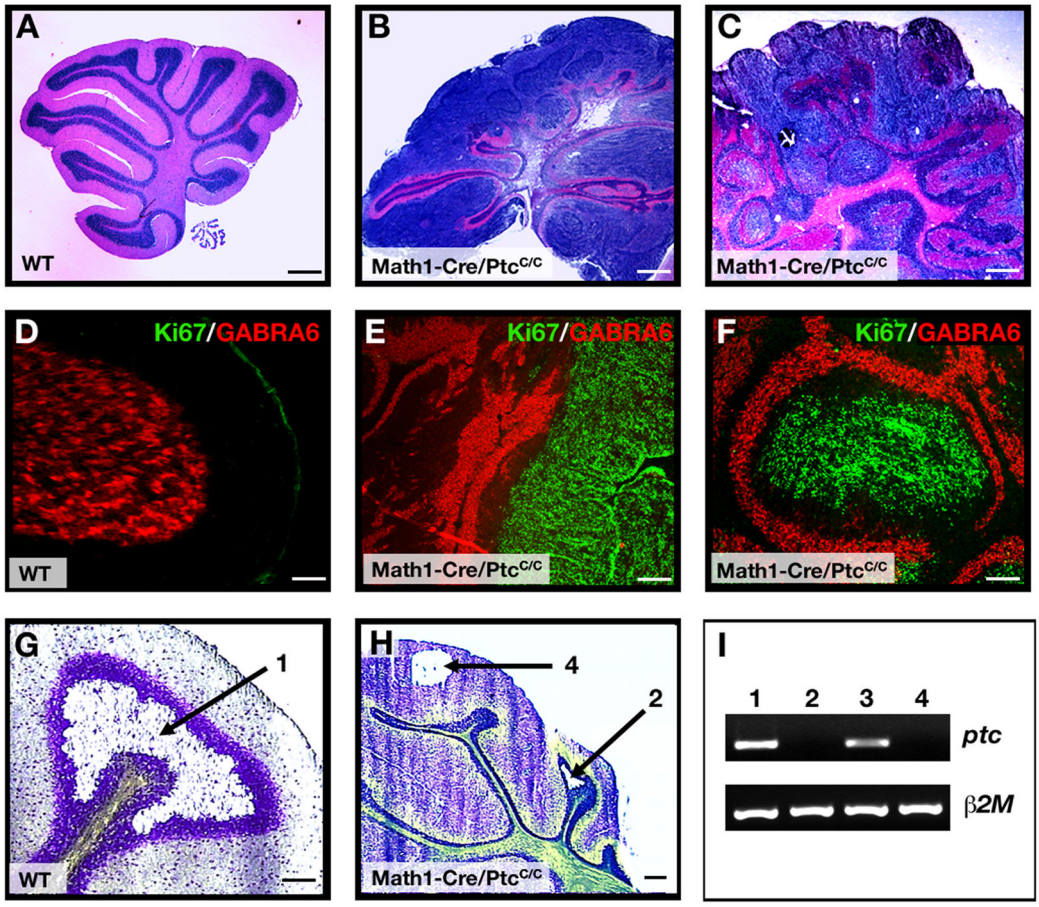

Figure 3. Most Math1-Cre/Ptc$^{C/C}$ GNPs differentiate despite loss of *ptc*

A–F. Cerebella from 6-week-old WT (A, D) and Math1-Cre/Ptc$^{C/C}$ mice (B, C, E, F) were stained with H&E (A–C) or with anti-Ki67 (green) to detect proliferation and anti-GABRA6 (red) to detect granule neuron differentiation (D–F). Whereas WT cerebella contain no proliferating cells (A, D), mutants exhibit extensive proliferation and differentiation, with proliferating cells either localized to the surface (B, E) or in nodules surrounded by differentiated cells (C, F). G–I. Cerebellar sections from 6-week-old WT (G) and Math1-Cre/Ptc$^{C/C}$ (H) mice were stained with cresyl violet, and the regions indicated by arrows were laser-captured for RNA analysis. I. RNA from WT IGL (lane 1, derived from region 1 in panel G), Math1-Cre/Ptc$^{C/C}$ IGL (lane 2, from region 2 in panel H), WT EGL (lane 3, tissue not shown) and proliferating cells at the surface of the Math1-Cre/Ptc$^{C/C}$ cerebellum (lane 4, from region 4 in panel H) were analyzed by RT-PCR for expression of *ptc* and *beta2-microglobulin* (β2m). Note the lack of *ptc* expression in mutant IGL (lane 2). Scale bars: panels A–C, 300 μm; panels D–H, 30 μm.

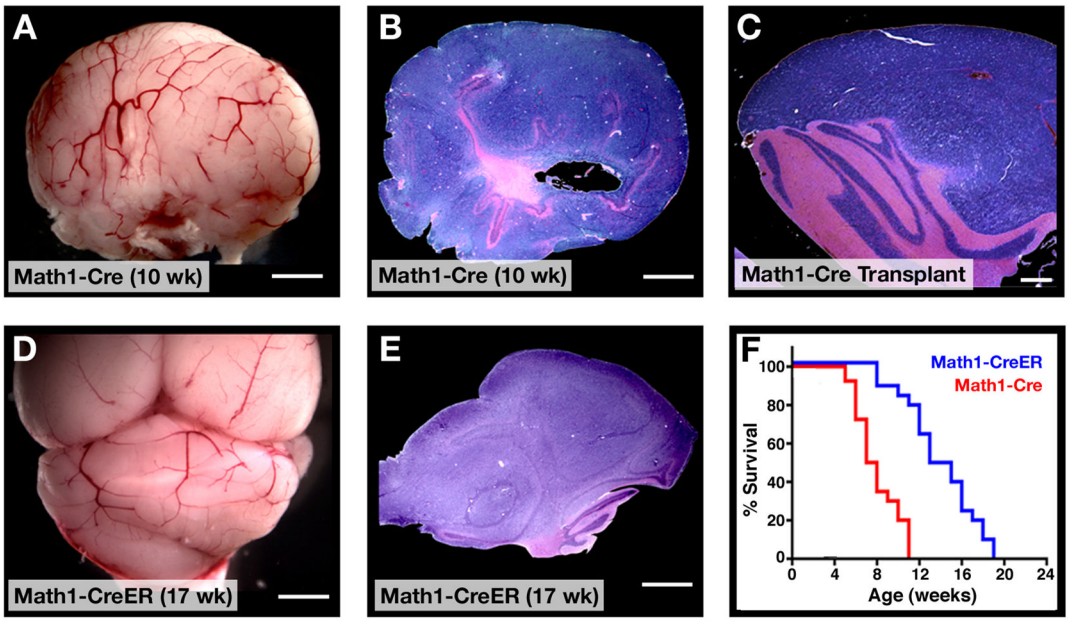

Figure 4. *ptc* deletion in GNPs leads to medulloblastoma

A–C. By 10 weeks of age, most Math1-Cre/Ptc$^{C/C}$ mice develop tumors. A. Cerebellum containing tumor. B. H&E-stained section of tumor. C. H&E-stained section of secondary tumor, induced by transplantation of Math1-Cre/Ptc$^{C/C}$ tumor cells into cerebellum of adult SCID-beige mouse. D–E. Postnatal deletion of *ptc* in GNPs results in medulloblastoma. Math1-CreER/Ptc$^{C/C}$ mice were treated with tamoxifen at P4 and sacrificed when symptoms developed (in this case at 17 weeks). Cerebella were photographed intact (D) or sectioned and stained with H&E (E). F. Survival curves for Math1-Cre/Ptc$^{C/C}$ mice (red) and Math1-CreER/Ptc$^{C/C}$ mice treated with tamoxifen at P4 (blue). Scale bars: 3mm (A, B, D and E); 400 μm (C).

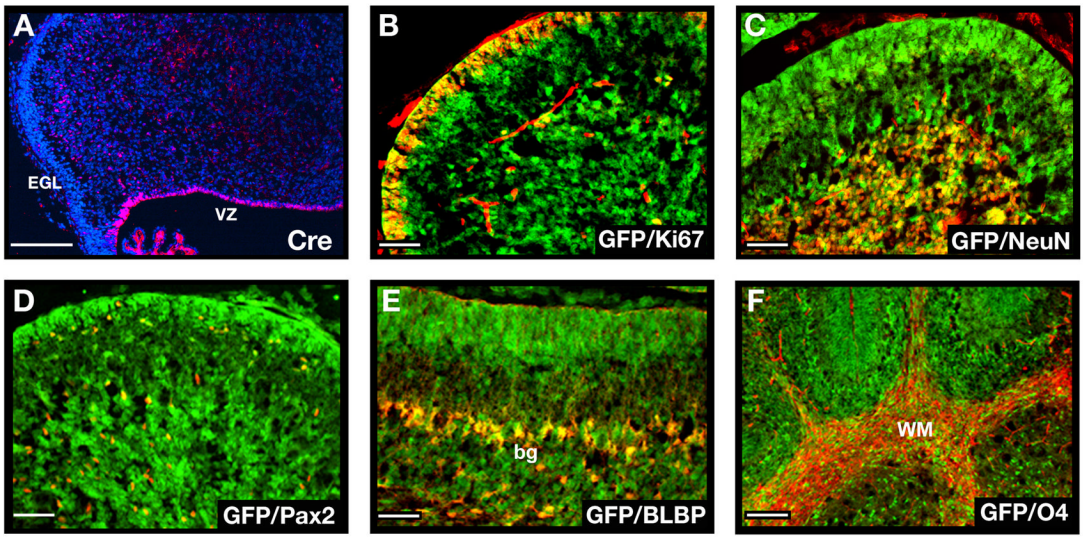

Figure 5. GFAP-Cre mice express Cre in neural stem cells

A. Cerebellar sections from E16.5 GFAP-Cre mice were stained with anti-Cre antibodies (red) and counterstained with DAPI (blue). Note the expression of Cre in the VZ but not in the EGL. B–F. Cerebellar sections from P8 GFAP-Cre/R26R-GFP mice (B–F) were stained with anti-GFP antibodies (green) to detect cells that had expressed Cre at some stage of development, and with antibodies specific for Ki67 to detect proliferating GNPs (B), NeuN to detect post-mitotic granule neurons (C), Pax2 to label interneuron progenitors (D), BLBP to label Bergmann glia (bg) and astrocytes (E) or O4 to detect oligodendrocytes in the white matter (WM, panel F). GFP was found to be co-expressed with each of these cell types (yellow staining in B–F). Scale bars represent 25 μm.

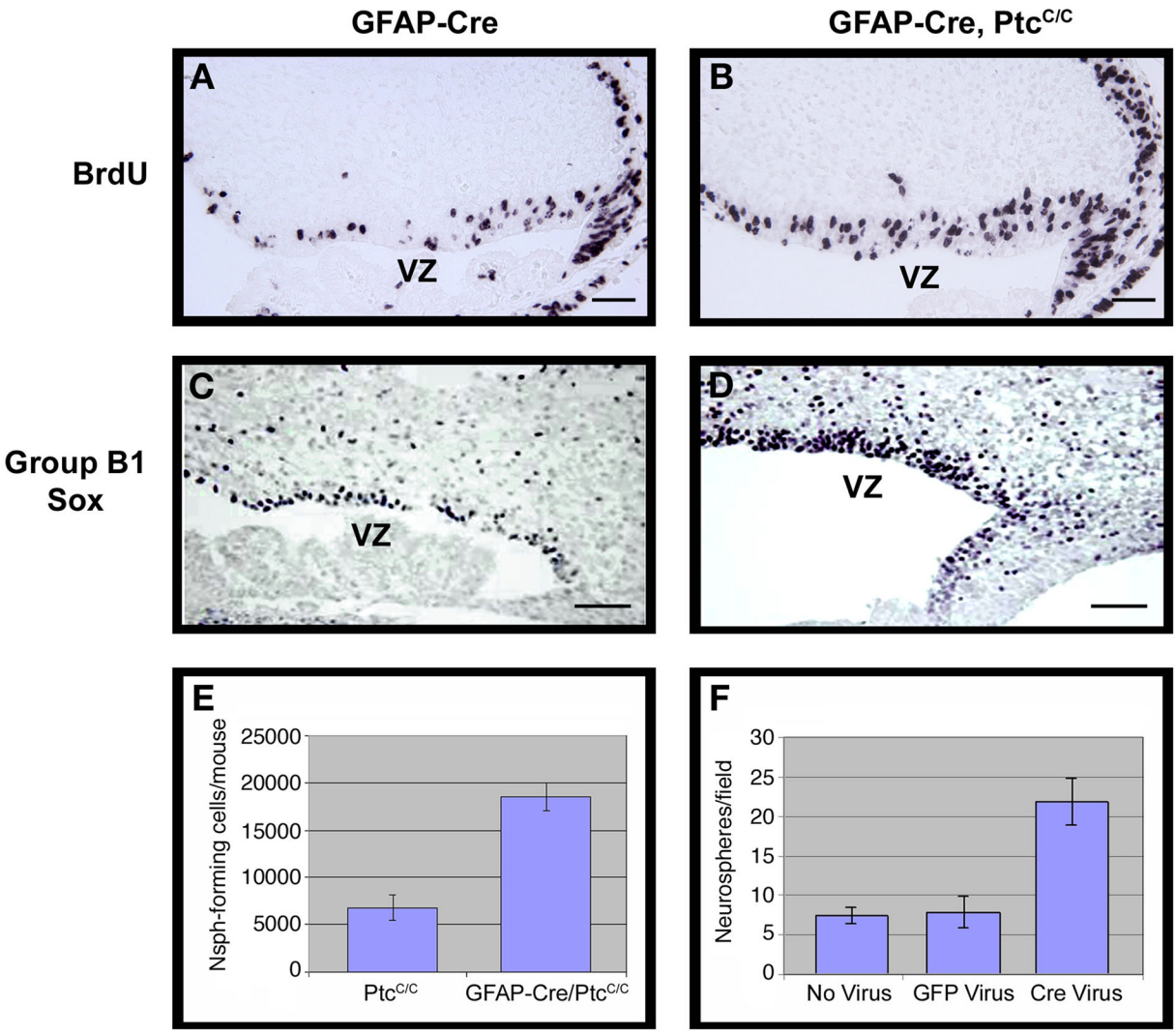

Figure 6. GFAP-Cre mediated deletion of *ptc* leads to expansion of NSCs

GFAP-Cre (A, C) and GFAP-Cre/Ptc$^{C/C}$ (B, D) embryos were pulsed with BrdU two hours before being sacrificed at E14.5. Brains were harvested and cerebellar sections stained with anti-BrdU (A, B) or anti-Group B1 Sox (C, D) antibodies. Cerebella from GFAP-Cre/Ptc$^{C/C}$ contained significantly more BrdU+ and SoxB1+ cells in the VZ. E–F. Deletion of *ptc* in embryonic cerebellar cells promotes increased neurosphere formation. E. Cerebella from E14.5 Ptc$^{C/C}$ and GFAP-Cre/Ptc$^{C/C}$ embryos were dissociated and cells were cultured at clonal density in neurosphere media. The number of neurospheres/mouse was calculated by multiplying the number of cells obtained from each embryo by the number of neurospheres observed in cultures from that embryo. Cerebella from GFAP-Cre/Ptc$^{C/C}$ mice yielded 2.7 times more neurospheres than those from Ptc$^{C/C}$ mice. F. Cells isolated from E14.5 Ptc$^{C/C}$ embryos were infected with no virus or with viruses carrying GFP or Cre-IRES-GFP. Infected (GFP+) cells were sorted and cultured at clonal density in neurosphere media. After 7 days, Cre-infected cells generated 2.8 times more neurospheres than GFP-infected cells and non-infected cells. Data in E and F represent means of triplicate samples ± SEM. Scale bars: 20 μm.

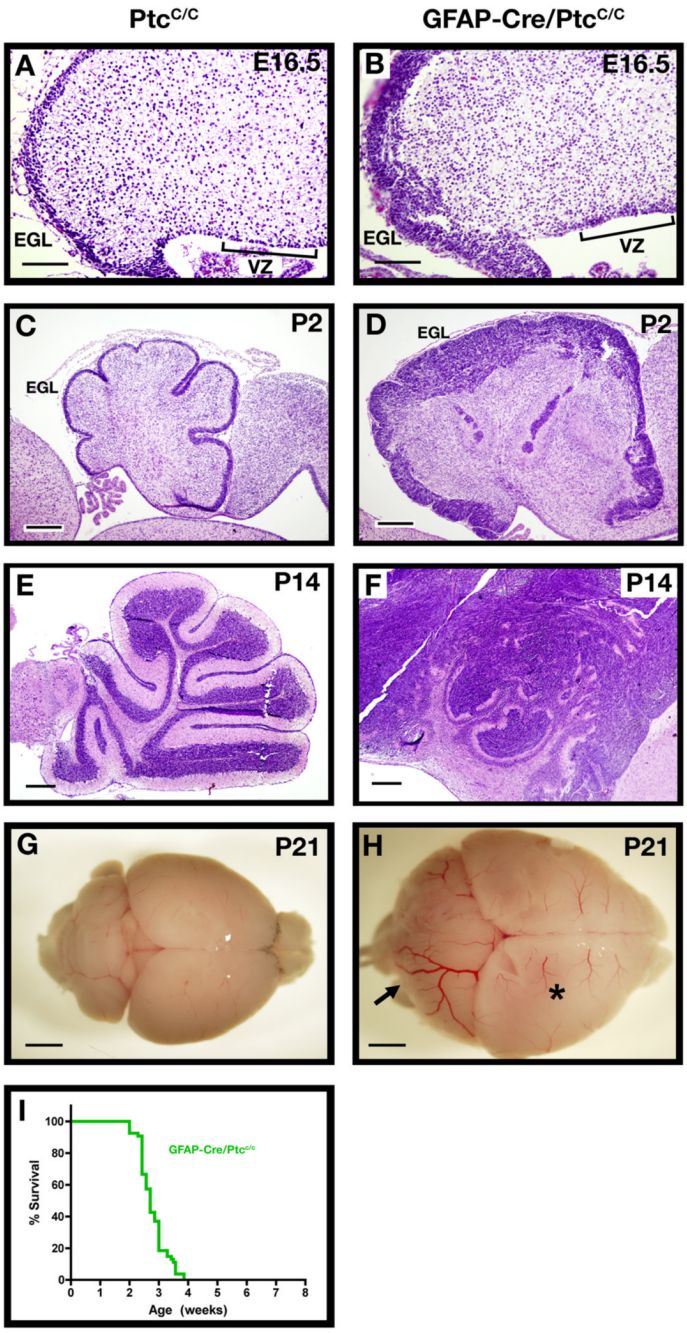

Figure 7. Deletion of *ptc* in NSCs results in rapid tumor formation

Cerebellar sections from $Ptc^{C/C}$ (A, C, E, G) and GFAP-Cre/$Ptc^{C/C}$ (B, D, F, H) mice were harvested and stained with H&E (A–F) or photographed whole-mount (G–H) at E16-P21. Note the expansion of both the VZ and EGL at E16.5 (A–B) and the persistent expansion of the EGL at postnatal ages (C–F). The arrow in H points to a tumor that has formed in the cerebellum. The forebrain (asterisk) in these animals also appears enlarged; histological examination (not shown) indicates that this is due to expansion of the ventricle (perhaps due to occlusion of cerebrospinal fluid circulation) rather than to increased growth or tumorigenesis in the cortex. I. Survival curve for GFAP-Cre/$Ptc^{C/C}$ mice. Scale bars: 20 μm (A and B); 100 μm (C and D); 300 μm (E and F); 2.5 mm (G and H).

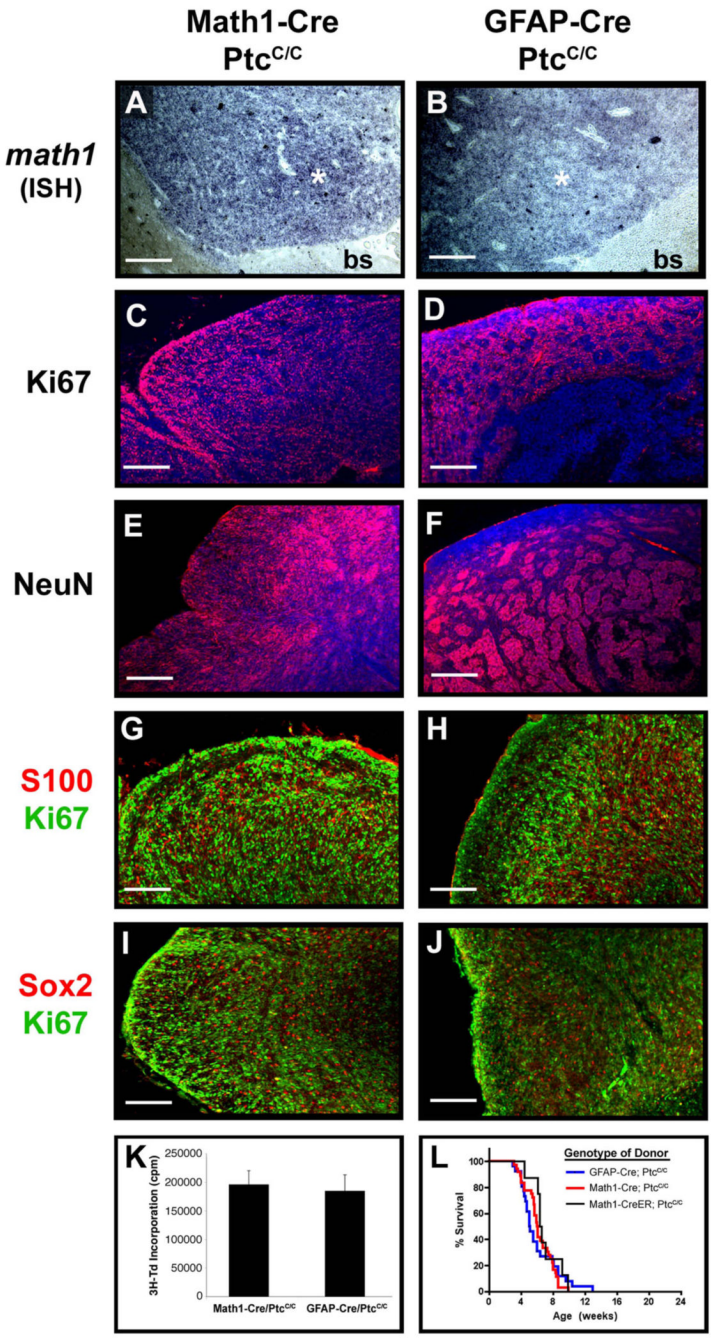

Figure 8. Tumors from Math1-Cre/Ptc$^{C/C}$ and GFAP-Cre/Ptc$^{C/C}$ mice display similar phenotypes

Sections from Math1-Cre/Ptc$^{C/C}$ (A, C, E, G and I) and GFAP-Cre/Ptc$^{C/C}$ (B, D, F, H and J) tumors were subjected to in situ hybridization to detect expression of *math1* (A, B) or stained with antibodies to detect proliferating cells (Ki67, C, D, G, H, I and J), differentiating neurons (NeuN, E and F), astrocytes (S100, G and H) and stem cells (Sox2, I and J). Sections in panels C–F were counterstained with DAPI (blue). In panels A and B, asterisk denotes tumor and "bs" indicates brainstem. K. Tumor Cells were cultured for 48h, pulsed with tritiated thymidine (^{3}H-Td), and harvested 18h later for measurement of thymidine incorporation. Data represent means of triplicate samples ± SEM. L. Survival curves of SCID-beige mice after transplantation of 1 × 10^6 tumor cells isolated from GFAP-Cre/Ptc$^{C/C}$ mice, Math1-Cre/Ptc$^{C/C}$ mice, and

Math1-CreER/Ptc$^{C/C}$ mice that had been treated with tamoxifen at P4. Scale bars represent 25 μm.